The C-terminal α-helix of YsxC is essential for its binding to 50S ribosome and rRNAs

Catherine Wicker-Planquart, Nicoletta Ceres, Jean-Michel Jault

Investigations on the C1q–Calreticulin–Phosphatidylserine Interactions Yield New Insights into Apoptotic Cell Recognition

Helena Païdassi[1]†, Pascale Tacnet-Delorme[1]†, Mélanie Verneret[1], Christine Gaboriaud[1], Gunnar Houen[2], Karen Duus[2], Wai Li Ling[1], Gérard J. Arlaud[1] and Philippe Frachet[1]*

[1]*Université Joseph Fourier Grenoble 1, Institut de Biologie Structurale Jean-Pierre Ebel, 38027 Grenoble, France; CNRS, Institut de Biologie Structurale Jean-Pierre Ebel, 38027 Grenoble, France; CEA, Institut de Biologie Structurale Jean-Pierre Ebel, 38027 Grenoble, France*
[2]*Department of Clinical Biochemistry and Immunology, Statens Serum Institut, DK-2300 Copenhagen, Denmark*

Both C1q and calreticulin (CRT) are involved in the recognition of apoptotic cells. CRT was initially characterized as a receptor for the C1q collagen-like fragment (CLF), whereas C1q was shown to bind apoptotic cells through its globular region (GR). Using purified CRT and recombinant CRT domains, we now provide unambiguous experimental evidence that, in addition to its CLF, the C1q GR also binds CRT and that both types of interactions are mediated by the CRT globular domain. Surface plasmon resonance analyses revealed that the C1q CLF and GR domains each bind individually to immobilized CRT and its globular domain with K_D values of (2.6–8.3) $\times 10^{-7}$ M. Further evidence that CRT binds to the C1q GR was obtained by electron microscopy. The role of CRT in the recognition of apoptotic HeLa cells by C1q was analyzed. The C1q GR partially colocalized with CRT on the surface of early apoptotic cells, and siRNA (small interfering RNA)-induced CRT deficiency resulted in increased apoptotic cell binding to C1q. The interaction between CRT and phosphatidylserine (PS), a known C1q ligand on apoptotic cells, was also investigated. The polar head of PS was shown to bind to CRT with a 10-fold higher affinity (K_D= 1.5 $\times 10^{-5}$ M) than that determined for C1q, and, accordingly, the C1q GR–PS interaction was impaired in the presence of CRT. Together, these observations indicate that CRT, C1q, and PS are all closely involved in the uptake of apoptotic cells and strongly suggest a combinatorial role of these three molecules in the recognition step.

**Corresponding author.* Equipe "Phagocytose du Soi Altéré," Institut de Biologie Structurale Jean-Pierre Ebel, 41 rue Jules Horowitz, 38027 Grenoble Cedex 1, France. E-mail address: philippe.frachet@ibs.fr.

† H.P. and P.T.D. contributed equally to this work.

Present address: H. Païdassi, Program of Development Immunology, Department of Pediatrics, Massachusetts General Hospital/Harvard Medical School, Boston 02114, MA, USA.

Abbreviations used: CRT, calreticulin; CLF, collagen-like fragment; GR, globular region; PS, phosphatidylserine; siRNA, small interfering RNA; plCRT, placental CRT; rCRT, recombinant CRT; SPR, surface plasmon resonance; ectoCRT, CRT exposed at the cell surface.

Introduction

The uptake of apoptotic cells by phagocytes is a physiological function that is essential for development and tissue homeostasis. In the healthy human, this results in most cases in an anti-inflammatory response and the induction of self-tolerance. This process is divided into several steps ranging from the recognition of altered cells to the acquisition of a new immunological status by the phagocyte (for reviews, see Refs. 1–4). Perturbation of this mechanism can lead to autoimmune diseases and to pathological inflammation. A number of molecules that either mark the apoptotic cell, serve as a receptor on macrophages, or bridge these two types of cells have been characterized, but the role of each of these partners, alone or in combination, remains to be fully elucidated.

Complement protein C1q and calreticulin (CRT) have been shown to be involved in apoptotic cell uptake. Over the past few years, a novel multifaceted role for the "old" protein C1q has emerged. Besides its role in the activation of the classical complement pathway in response to pathogen infection, C1q plays a crucial role in the detection and scavenging of a wide variety of noxious altered-self substances, such as β-amyloid fibrils, the pathological form of the prion protein, apoptotic and necrotic cells, or modified forms of the low-density lipoprotein.[5–11] Interestingly, unlike the other complement proteins, C1q is produced by macrophages and immature dendritic cells. Numerous studies have shown that C1q influences the phagocyte "status" through regulation of cytokine expression[12,13] and that it may be involved in the nonimmunogenic presentation of self-antigens through its ability to modulate maturation of dendritic cells.[14–18] C1q acts as a bridging molecule that binds apoptotic cells through interactions between its globular regions (GRs) and various molecules, probably not yet all characterized, that become surface-exposed under apoptotic stress conditions and contribute "eat-me" signals. Among these molecules are the emblematic apoptosis marker phosphatidylserine (PS)[19] and DNA exposed at the surface of apoptotic cells.[20–22] The multifunctional CRT protein,[23–25] a calcium-binding chaperone protein mainly located in the endoplasmic reticulum, is now considered an early eat-me signal that enhances phagocytosis of apoptotic cells and, when exposed on cancer cells, elicits an immunogenic response.[26,27] The observation that CRT could be involved in processes with opposite (immunogenic *versus* nonimmunogenic) consequences reflects the complexity of the pathways that regulate the global response to the recognition of altered-self cells, suggesting a possible combinatorial interplay of soluble molecules and receptors contributed by the phagocyte and its target.

CRT is also known to act as a "receptor for the C1q collagenous domain" (cC1qR) at the surface of phagocytes in conjunction with its co-receptor CD91/LRP (lipoprotein receptor-related protein).[28–30] Binding of CRT to the C1q GR has also been suggested by several studies even though this interaction has not been fully established.[31–34] Again, these observations evoke a double play for this protein as both a phagocyte receptor and an eat-me signal on the apoptotic cell surface.

In light of these observations and considering the crucial role of CRT and of C1q-mediated phagocytosis in the control of the immune response, we have further investigated the CRT–C1q interactions and their implications in the uptake of apoptotic cells. Using placenta-derived and recombinant forms of CRT, we provide unambiguous evidence of the ability of C1q GR to bind to the CRT globular domain. A small interfering RNA (siRNA)-based strategy leading to a decrease in surface-exposed CRT also reveals that CRT modulates C1q binding to apoptotic cells, very likely by competing with this protein for interaction with PS. These findings shed new light on the role of C1q and CRT and their possible coordination in the elimination of apoptotic cells.

Results

Production and purification of recombinant CRT and its globular and P domains

Expression vectors for the P and globular domains of CRT were constructed from the pHFX-CRT plasmid (Fig. 1a). For the P domain, regions coding for the CRT N- and C-terminal domains (residues 1–188 and 289–400, respectively) were deleted. The globular domain was obtained by fusing the CRT N-terminal (residues 1–187) and C-terminal (residues 285–400) domains by means of a three-amino-acid linker (GSG) as a substitute for the P domain. This latter construct retains a larger part of the original protein than the N/C domain comprising a 15-residue linker produced previously by Tan *et al.*[35] (Fig. 1a). The expression vectors used allowed production of the recombinant proteins fused to a histidine affinity tag. SDS-PAGE analysis of the purified recombinant proteins indicated that full-length CRT, its globular domain, and its P domain were essentially pure and exhibited apparent molecular masses of 55, 40 and 23 kDa, respectively, under reducing conditions (Fig. 1b). The corresponding molecular masses determined by matrix-assisted laser desorption/ionization time-of-flight (MALDI-TOF) analysis were 49,431 ± 50, 38,111 ± 40, and 14,756 ± 15 Da, respectively, consistent with the values predicted from the amino acid sequences after removal of the N-terminal methionine (49,399, 38,114, and 14,752 Da, respectively). That the recombinant proteins were

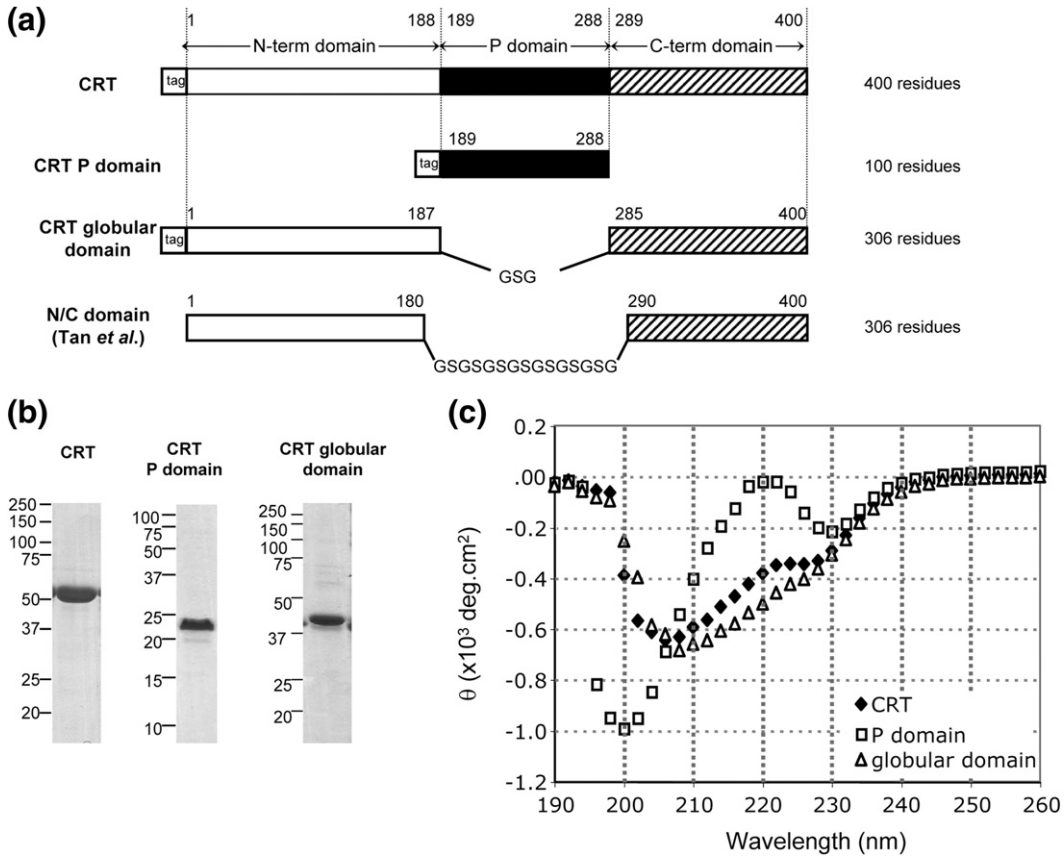

Fig. 1. Design and characterization of recombinant human CRT domains. (a) Schematic representation of the CRT constructs used in this study. The N/C domain produced by Tan *et al*. is shown for comparison. (b) SDS-PAGE analysis of full-length CRT, the CRT P domain, and the CRT globular domain fused to HAT, expressed in *E. coli* BL21. All samples were analyzed under reducing conditions and stained with Coomassie blue. The positions of molecular mass markers (expressed in kilodaltons) are shown. (c) Far-UV CD spectra (260–190 nm) of the CRT constructs at 25 °C.

folded was assessed by circular dichroism (CD) spectroscopy. The far-UV spectrum of recombinant CRT (rCRT) was characterized by a minimum at 208 nm, indicative of the presence of α-helix, and a prominent shoulder at 229 nm (Fig. 1c), in keeping with a previous report by Li *et al*.[36] The globular domain exhibited a marked minimum at 209 nm as observed previously for a similar N/C construct.[35] In contrast, the P domain yielded a strikingly different spectrum, with two strong minima at 200 and 230 nm.[31–34] These analyses strongly suggested that the three recombinant proteins were properly folded. In addition, all recombinant forms of CRT were found to be monomeric and nonaggregated as judged by size-exclusion chromatography (data not shown), in concordance with published data by Young and collaborators.[37]

C1q, its CLF, and its GR bind CRT

Whether interaction of C1q with CRT involves its GR, CLF, or both domains is still a controversial issue.[31–34,38,39] To further investigate this question, the C1q–CRT interaction was analyzed by surface plasmon resonance (SPR) using human placental (plCRT) or rCRT immobilized on a sensor chip and intact C1q, its GR, or its CLF as soluble ligands. As illustrated in Fig. 2, intact C1q and its GR and CLF all bound to immobilized plCRT. The kinetic parameters of CRT recognition were determined by recording sensorgrams at varying C1q, GR, and CLF concentrations (Fig. 2a–c). For the C1q GR and CLF, the kinetic (k_a, k_d) and dissociation (K_D) constants were calculated with a simple 1:1 Langmuir binding model (Table 1). The C1q GR and CLF bound plCRT with similar K_D values of 3.8×10^{-7} and 2.6×10^{-7} M, respectively. However, the CLF had significantly higher k_a and k_d values than the GR, as illustrated in the sensorgrams in Fig. 2d. Similar experiments were performed with rCRT as the immobilized ligand, again demonstrating efficient recognition by both the C1q CLF and the GR (Table 1). Both C1q domains bound rCRT with K_D values slightly higher than but nevertheless in the same order as those determined for plCRT. As observed for plCRT, the C1q CLF also had higher k_a

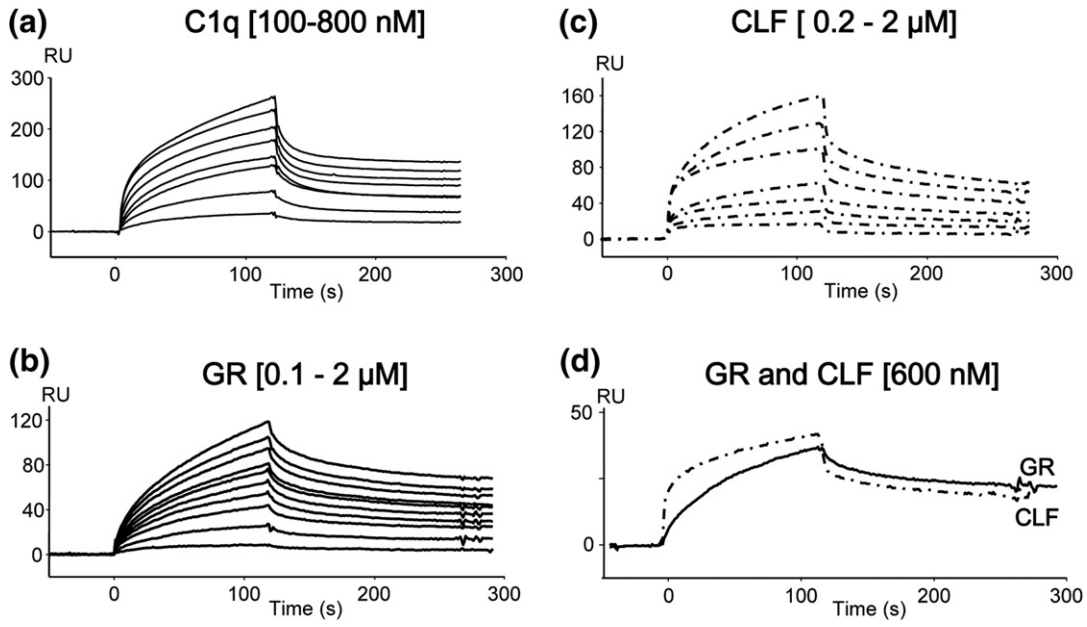

Fig. 2. SPR analysis of the interaction of C1q and its fragments with plCRT. Binding of intact C1q (a), C1q GR (b), and C1q CLF (c) to immobilized plCRT. (d) Comparison of the C1q GR and CLF sensorgrams at the same concentration (600 nM). All interactions were measured at a flow rate of 20 μl/min. Association and dissociation curves were recorded for 120 s. The concentrations of soluble ligands were as follows: C1q: 100, 200, 300, 400, 500, 600, and 800 nM; GR: 0.1, 0.2, 0.4, 0.5, 0.8, 1.0, 1.2, 1.4, 1.6, and 2.0 μM; CLF: 0.2, 0.4, 0.6, 1.0, 1.6, and 2.0 μM. All other conditions are described under Materials and Methods.

and k_d values than the GR. Intact C1q itself was found to bind to both plCRT and rCRT with higher affinities ($K_D = 1.6 \times 10^{-7}$ and 1.2×10^{-7} M, respectively) than its GR or CLF (Table 2). Proper kinetic analysis of these interactions required the use of a two-state reaction binding model. This model takes into account complex conformational changes, leading to an increasingly more stable complex formed in two steps and fitting the equation $A + B \Leftrightarrow AB \Leftrightarrow AB^*$. The two groups of kinetic constants and the resulting apparent affinity constant (K_D), calculated by the BIAeval software, are listed in Table 2. The fact that the experimental binding data can be properly fitted using this model strongly suggests that CRT recognition by intact C1q implies (a) conformational changes that do not take place in the isolated GR or CLF domains. According to the kinetic analysis using this two-state model, rCRT and plCRT have similar interaction properties with C1q (Table 2), indicating that rCRT is produced in a fully functional state. Of note, the K_D values of the interaction with full-length CRT or the CRT globular domain were significantly lower for intact C1q compared to its GR (Tables 1 and 2), accounting for an increased binding avidity of C1q arising from its hexameric structure and/or from conformational changes during the binding process.

Electron microscopy was next used with a view to observing the interaction between C1q and rCRT. Because CRT and the C1q GRs have similar molecular masses, rCRT was specifically labeled with nickel(II)–nitrilotriacetic acid–Nanogold®

Table 1. Kinetic constants for the interaction between C1q GR or C1q CLF and CRT or its globular domain

	Soluble analyte					
	C1q GR			C1q CLF		
Immobilized ligand	K_a (M^{-1} s^{-1})	K_d (s^{-1})	K_D (M)	K_a (M^{-1} s^{-1})	K_d (s^{-1})	K_D (M)
plCRT	$6.2 \pm 1.3 \times 10^3$	$2.4 \pm 0.2 \times 10^{-3}$	$3.8 \pm 1.0 \times 10^{-7}$	$1.3 \pm 0.9 \times 10^4$	$3.4 \pm 0.6 \times 10^{-3}$	$2.6 \pm 1.4 \times 10^{-7}$
Recombinant CRT	$2.4 \pm 0.5 \times 10^3$	$2.0 \pm 0.1 \times 10^{-3}$	$8.3 \pm 1.2 \times 10^{-7}$	$7.9 \pm 1.0 \times 10^3$	$3.1 \pm 0.1 \times 10^{-3}$	$3.9 \pm 0.8 \times 10^{-7}$
CRT globular domain	$2.4 \pm 0.7 \times 10^3$	$1.7 \pm 0.1 \times 10^{-3}$	$7.0 \pm 2.3 \times 10^{-7}$	$3.5 \pm 1.4 \times 10^3$	$1.7 \pm 0.1 \times 10^{-3}$	$4.8 \pm 2.0 \times 10^{-7}$

Binding of C1q GR (0.1–2 μM) and CLF (0.2–2 μM) was measured as described under Materials and Methods. The association (k_a) and dissociation (k_d) rate constants were determined with a 1:1 Langmuir binding model. Values are the means of at least three separate experiments.

Table 2. Kinetic constants for the binding of full-length C1q to CRT and its globular domain

	Soluble analyte				
	C1q				
Immobilized ligand	K_{a1} (M^{-1} s^{-1})	K_{d1} (s^{-1})	K_{a2} (s^{-1})	K_{d2} (s^{-1})	K_D (M)
plCRT	$11 \pm 4 \times 10^3$	$3.8 \pm 1.1 \times 10^{-2}$	$2.0 \pm 0.7 \times 10^{-2}$	$8.1 \pm 6.3 \times 10^{-4}$	$1.6 \pm 1.5 \times 10^{-7}$
rCRT	$6.3 \pm 0.6 \times 10^3$	$2.4 \pm 0.5 \times 10^{-2}$	$1.7 \pm 0.6 \times 10^{-2}$	$5.3 \pm 0.5 \times 10^{-4}$	$1.2 \pm 0.5 \times 10^{-7}$
CRT globular domain	$6.2 \pm 2 \times 10^3$	$1.9 \pm 0.1 \times 10^{-2}$	$2.2 \pm 0.1 \times 10^{-2}$	$3.7 \pm 2.9 \times 10^{-4}$	$0.52 \pm 0.6 \times 10^{-7}$

Binding of C1q (0.05–0.8 μM) was measured as described under Materials and Methods. The association (k_{a1}, k_{a2}) and dissociation (k_{d1}, k_{d2}) rate constants were determined by global fitting of the data using a two-state reaction binding model. The dissociation constants K_D were determined from the $(k_{d1}/k_{a1})(k_{d2}/k_{a2})$ ratios. The values shown for plCRT and rCRT are the means of three separate experiments.

beads, a reagent that has a high affinity for the multiple histidine residues contained in the histidine affinity tag (HAT) fusion of rCRT. As illustrated in Fig. 3, gold-labeled rCRT specifically bound to the GR of C1q. In some cases (Fig. 3c, i and ii), attachment through the C1q CLF region was also observed. In full agreement with the SPR binding experiments, these analyses thus provided further evidence of the ability of CRT to interact with both the C1q CLF and the GR domains.

CRT interacts with C1q through its globular domain

To gain insight into the area of the CRT molecule involved in C1q recognition, the rCRT globular domain and P domain were immobilized covalently on a sensor chip and allowed to interact with soluble C1q, its GR, or its CLF (Fig. 4). Using the P domain, we detected no significant interaction with any of the C1q domains. In contrast, the CRT globular domain was found to bind C1q, its GR, and its CLF in a manner similar to that of full-length rCRT. For interaction between the immobilized CRT globular domain and C1q, again the two-state reaction binding model provided the best global fit (Table 2). The resulting apparent affinity constant [$(0.52 \pm 0.6) \times 10^{-7}$ M] was in the same range as that measured for rCRT [$(1.2 \pm 0.5) \times 10^{-7}$ M]. As expected, binding of C1q GR and CLF to the CRT globular domain obeyed a simple 1:1 Langmuir binding model (Table 1). Again, the kinetic parameters

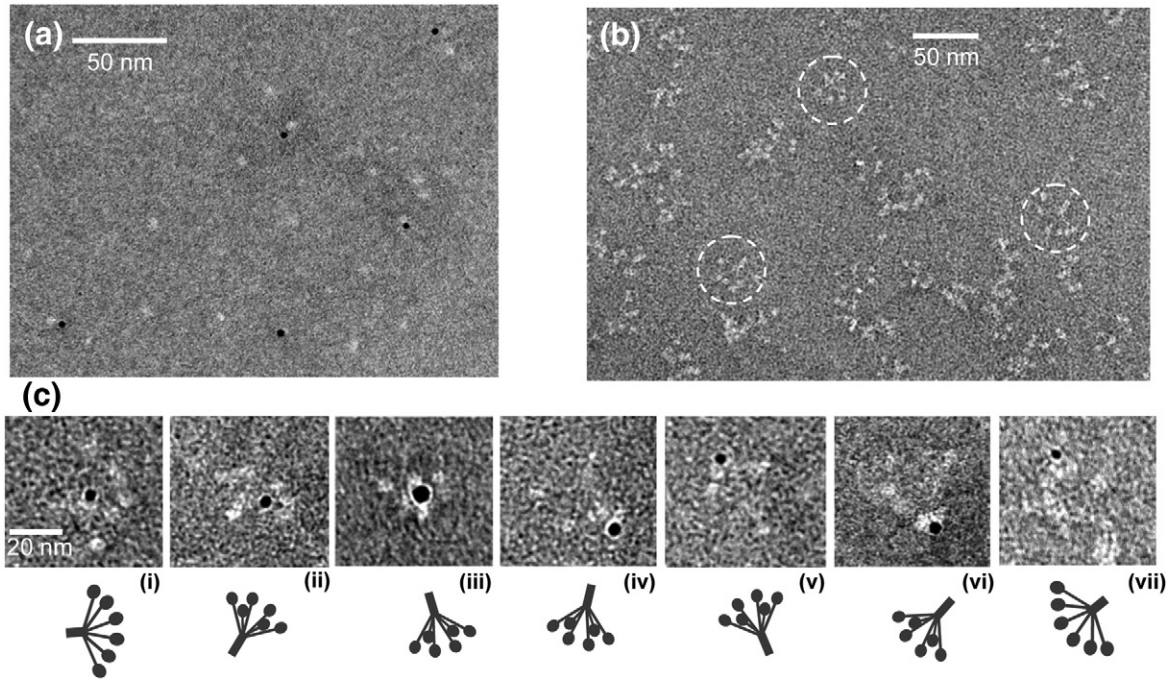

Fig. 3. Electron microscopy images of the interaction between gold-labeled CRT and C1q. (a) Representative micrograph of gold-labeling beads incubated with CRT molecules alone. All gold beads were attached to CRT molecules. (b) Representative area of gold-labeling beads incubated with C1q molecules alone. No gold beads were observed. Some representative C1q molecules are circled. (c) Gold-labeled CRT molecules bound to individual C1q molecules. Attachment through both the GR (iii–vii) and the CLF (i, ii) domains were observed.

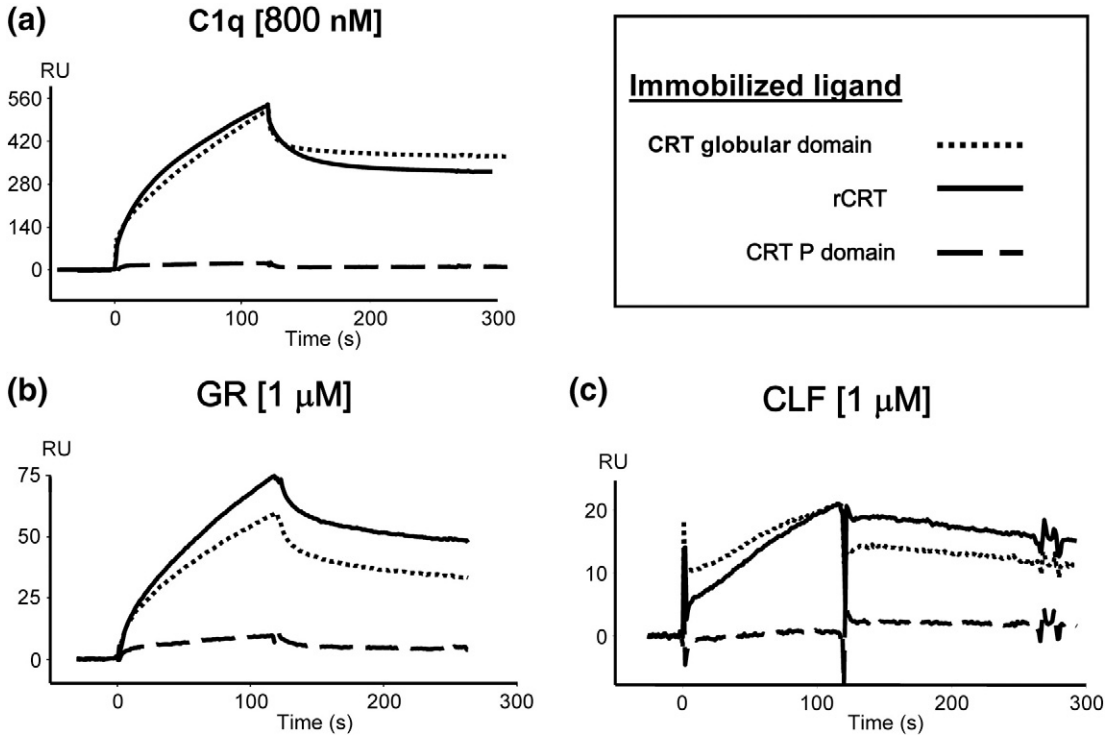

Fig. 4. Interaction of C1q and its GR and CLF with rCRT and its domains. Binding of C1q (a), C1q GR (b), and C1q CLF (c) to immobilized rCRT, the CRT globular domain, and the CRT P domain. In each case, the same amount of proteins was immobilized on the sensor chip. The kinetic parameters of the interactions determined by recording sensorgrams at varying C1q, C1q GR, and C1q CLF concentrations are listed in Tables 1 (C1q GR and CLF) and 2 (C1q).

were similar to those measured for full-length CRT (Table 1). Together, these results provided clear evidence that the CRT globular domain mediates the interaction with C1q through its ability to bind to both the C1q GR and the CLF domains.

C1q GR partially colocalizes with CRT on the surface of apoptotic HeLa cells

Our finding of the C1q ability to bind CRT through its GR prompted us to investigate whether CRT could be involved as a ligand in the recognition of apoptotic cells by C1q. To this end, CRT exposed at the cell surface (ectoCRT) was analyzed on viable and early apoptotic HeLa cells. Apoptosis was induced by UV-B irradiation and monitored as described previously.[19] Viable and apoptotic cells were then analyzed by flow cytometry using anti-CRT antibodies. As shown in Fig. 5a, CRT was detected at the surface of viable HeLa cells, and the staining increased for early apoptotic cells (analyzed 2 and 4 h after UV-B irradiation) but remained unchanged up to 6 h after induction of apoptosis (data not shown). As shown previously,[19] cells had not undergone significant necrosis at this stage. Thus, as reported previously for Jurkat cells and neutrophils,[26] CRT exposure at the surface of HeLa cells increases significantly during apoptosis. Confocal laser microscopy was next used to analyze the distribution of ectoCRT and bound C1q GR on the surface of early apoptotic cells. As illustrated in Fig. 5b, double immunofluorescence labeling showed that C1q GR colocalized to a large extent with ectoCRT in certain areas of the surface of early apoptotic cells (overlay, lower panel). In contrast, C1q GR and ectoCRT were clearly not superimposed on the surface of nonapoptotic cells (overlay, upper panel). These observations, together with our previous finding that C1q recognizes CRT through its GR, suggested that a direct C1q GR–CRT interaction occurred in newly organized membrane patches on the apoptotic cell surface.

Inhibition of CRT expression increases binding of apoptotic cells to C1q

To further investigate the implication of CRT in the recognition of apoptotic cells by C1q, we used an RNA interference strategy to inhibit CRT expression. As illustrated in the representative experiment shown in Fig. 6a, CRT knockdown using a specific siRNA efficiently reduced exposure of CRT at the surface of HeLa cells, resulting in decreases of 49–79%, 48 h after siRNA transfection. Apoptotic or viable CRT-deficient cells were then tested for their ability to bind to immobilized C1q using a SPR-

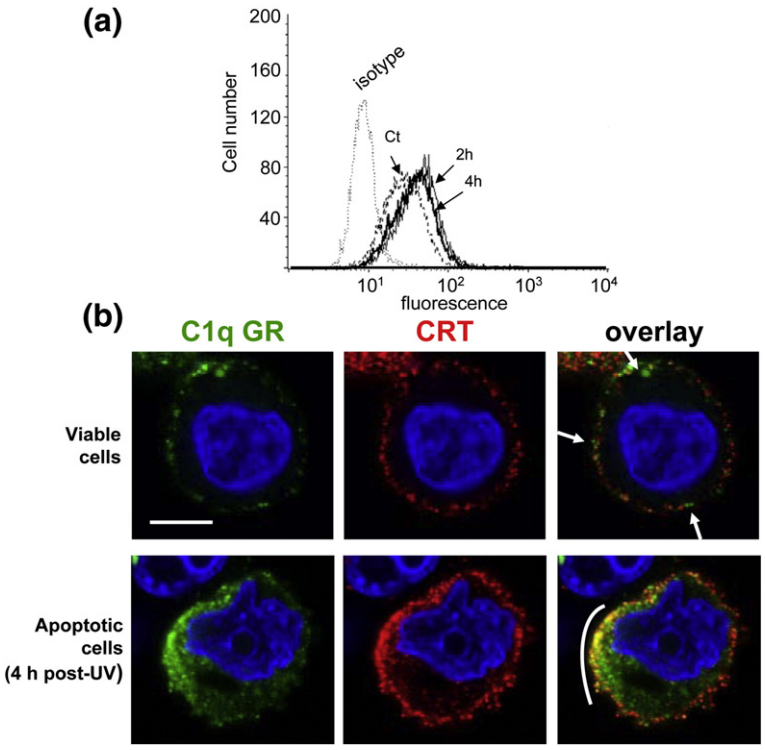

Fig. 5. C1q GR partially colocalizes with surface-exposed CRT on early apoptotic cells. (a) CRT cell-surface expression was assessed with a monoclonal anti-CRT antibody by FACS (fluorescence-activated cell sorting) analysis on viable (Ct) and early apoptotic HeLa cells (2 and 4 h after UV-B irradiation). (b) Cells were submitted to a double-immunofluorescence labeling for C1q GR (green) and CRT (red) followed by confocal laser microscopy detection as described under Materials and Methods. Nuclei were labeled with Hoechst (blue). White arrows show labeling disjunctions in viable HeLa cells (upper panels). The white bow indicates areas where C1q GR colocalizes with CRT in early apoptotic cells (lower panels). The scale bar represents 10 μm.

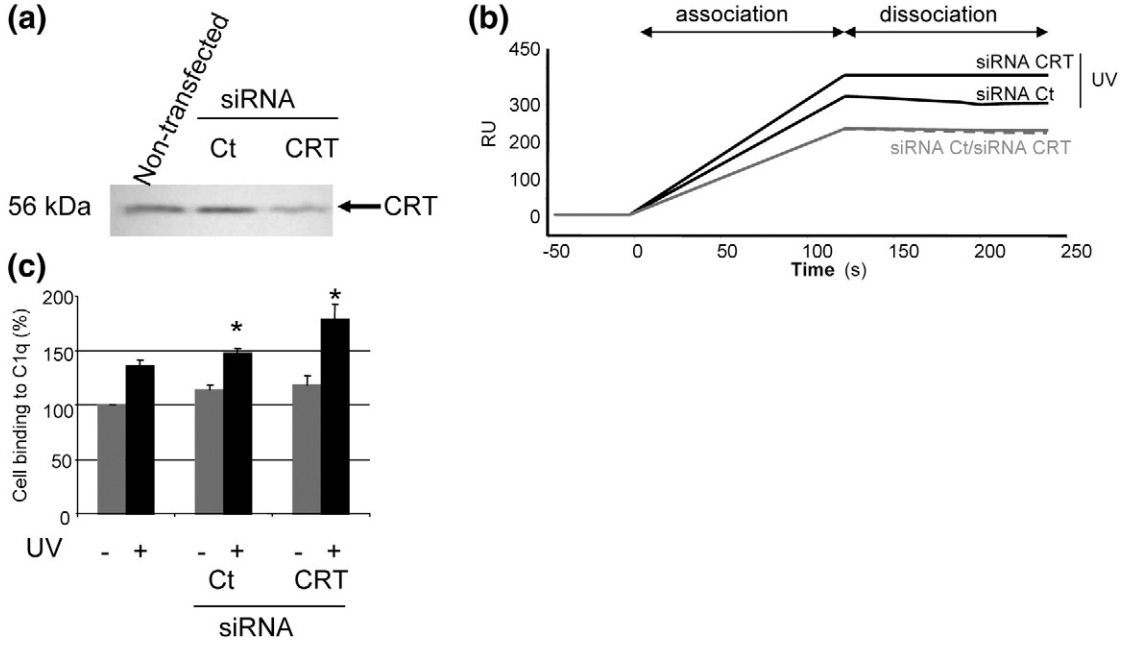

Fig. 6. Effect of CRT knockdown on cell binding to C1q. (a) CRT exposed on the surface of untreated or siRNA-treated HeLa cells was analyzed by SDS-PAGE analysis and immunobloting as described under Materials and Methods. (b) Viable or UV-B-irradiated HeLa cells (2 h after UV-B irradiation) treated with CRT-specific or control siRNA were harvested, suspended at 2.5×10^5 cells/ml in 140 mM NaCl, 5 mM KCl, 1 mM $MgCl_2$, 2.5 mM $CaCl_2$, and 25 mM Hepes (pH 7.4) containing 0.005% surfactant P20 and then passed over a C1q-coated sensor chip at a flow rate of 10 μl/min. Association and dissociation were both monitored for 120 s. (c) The results of the experiments shown in (b) are expressed relative to the capture of viable and apoptotic cells by C1q in the absence of siRNA treatment. Data represent the mean ± SD of three independent experiments. $*P < 0.005$; significance was determined by Student's t test.

based assay developed in previous studies.[19,20] siRNA-treated or untreated HeLa cells were rendered apoptotic by UV-B irradiation, and then both control cells and early apoptotic cells (2 h after irradiation) were allowed to bind immobilized C1q. As already reported in our previous study,[19] apoptosis induced a marked increase in cell capture by C1q (Fig. 6b). Treatment with a control siRNA had no significant effect on the capture of viable or apoptotic cells (Fig. 6b and c). In contrast, whereas transfection with CRT specific siRNA had no effect on the capture of viable cells, this treatment increased binding of apoptotic cells to C1q by >31%. At first sight, this result was difficult to reconcile with our previous observations, since a decrease in cell capture by C1q, rather than an increase, would have been expected. This suggested that despite the ability of C1q to bind CRT, recognition of apoptotic cells involves more complex mechanisms.

CRT associates with PS and thereby inhibits the C1q GR–PS interaction

Considering that PS, a known ligand of the C1q GR domain,[19] had been shown to colocalize with CRT in patches on apoptotic cell membranes,[26] this raised the possibility of an interaction between CRT and PS. To test this hypothesis, we first analyzed the binding of a water-soluble derivative (06:0 PS) composed of the polar moiety of PS connected to two six-carbon saturated hydrocarbon chains. As illustrated in Fig. 7a, SPR analysis at varying concentrations of this ligand revealed a dose-dependent interaction with immobilized rCRT. The kinetic rate constants of the interaction were estimated at 22.2 M^{-1} s^{-1} (k_a) and 3.38×10^{-4} s^{-1} (k_d), with a resulting K_D of about 1.5×10^{-5} M, a value approximately 10-fold lower than that determined in our previous study for the interaction between 06:0 PS and immobilized C1q ($K_D=1.7\times10^{-4}$ M).[19] Further analyses were performed to test the CRT-binding ability of the water-soluble derivatives of phosphatidylcholine (06:0 PC) and phosphatidylethanolamine (06:0 PE). As illustrated in Fig. 7b, neither of these derivatives interacted significantly with immobilized CRT at concentrations up to 6 mM, providing evidence for the specificity of CRT for the polar head of PS.

We next used a co-sedimentation assay to investigate the effect of CRT on the binding of C1q GR to PS vesicles; the extent of interaction was assessed from the relative amount of C1q GR associated with the vesicles in the pellet after centrifugation.[19] As shown in Fig. 7c, the C1q GR readily bound to the PS vesicles in the absence of CRT, the whole C1q GR

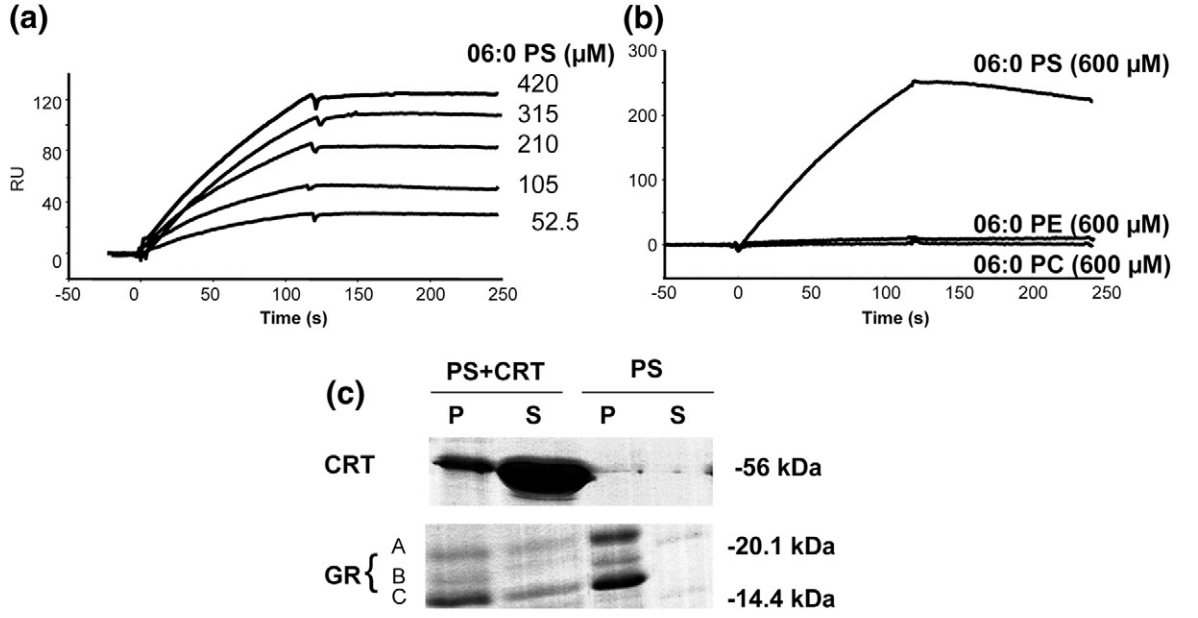

Fig. 7. CRT binds to PS, thereby inhibiting the C1q–PS interaction. (a) SPR analysis of the interaction between immobilized rCRT and soluble 06:0 PS. All interactions were measured in the running buffer (PBS, 1 mM $CaCl_2$, pH 7.4) at a flow rate of 10 μl/min. Association and dissociation curves were each recorded for 120 s. The concentrations of the soluble 06:0 PS ligand are shown. (b) Comparative SPR analyses of the interaction of 06:0 PS, 06:0 PC, and 06:0 PE to immobilized CRT. (c) Analysis by co-sedimentation of the interaction between the C1q GR and the PS vesicles: effect of CRT. PS vesicles were incubated in the presence or absence of rCRT and allowed to interact with C1q GR. After ultracentrifugation, the pellet (P) and supernatant (S) fractions were separated, and their relative GR content was assessed by SDS-PAGE analysis as described under Materials and Methods. Molecular weight markers are indicated on the right. Data are representative of three independent experiments.

material being found in the pellet. In contrast, preincubation of the vesicles with CRT significantly decreased the amount of C1q GR associated with the vesicles. In addition, part of the CRT was found to co-sediment with the PS vesicles, providing further evidence for a CRT–PS interaction. Based on these observations, it became clear that CRT had the ability to bind PS and thereby to competitively inhibit the C1q GR–PS interaction.

Discussion

A number of studies indicate that both C1q and ectoCRT are involved in the recognition of apoptotic cells. CRT was initially characterized as a C1q receptor through its ability to interact with its collagen region (CLF), whereas it was observed more recently that the C1q GRs are responsible for the binding of C1q to apoptotic cells. The objective of this study was to further investigate the C1q–CRT interactions at the molecular and cellular levels to better understand how these interactions contribute to the phagocytosis of altered-self cells.

First, this study provides unambiguous experimental evidence that, in addition to its CLF, the GR of C1q also binds to CRT, both types of interactions being mediated by the CRT globular domain. These conclusions are based on the following observations: (i) As shown by SPR analyses, the C1q GR and CLF domains recognize CRT with similar affinities (K_D values = $(2.6–8.3) \times 10^{-7}$ M). That CRT binds to the GR of C1q is further supported by electron microscopy images providing direct evidence of such an interaction. (ii) A rCRT globular domain corresponding to the N-terminal domain fused to the C-terminal domain, and excluding the P domain, is as efficient as the full-length molecule for binding to C1q and its GR and CLF domains. The rCRT globular domain (residues 1–187 fused by a three-residue linker to residues 285–400) and CRT P domain (residues 189–288) produced in this study were designed to preserve the CRT structural domain limits as deduced from homology with the chaperone calnexin and from NMR analysis of individual CRT domains.[40,41] We found that the P domain did not significantly interact with C1q, in contrast with previously published data.[33,38] This discrepancy possibly arises from the fact that the P domain used in these latter studies partly overlaps the CRT globular domain, or from the use of short peptides from the P domain. However, we cannot exclude that in the context of full-length CRT, C1q could make secondary interactions with residues in the P domain.

Interestingly, SPR kinetic analyses of the binding of full-length C1q to CRT were shown to fit a two-state reaction binding model, strongly suggesting that this interaction implies a conformational change in C1q. This observation is in line with the data published by Steino and collaborators,[34] who studied CRT binding to C1q immobilized on a polystyrene surface. Their results suggested that immobilization induces a C1q conformational change and that this change allows CRT to bind C1q, initially to its CLF and then subsequently to its GR. That C1q needs conformational changes to bind CRT is also supported by the observation that CRT binding was not observed on SPR experiments when C1q was covalently immobilized.

We also analyzed exposure of CRT at the surface of HeLa cells and the role of this ectoCRT in the recognition of early apoptotic cells by C1q. CRT was found to be present on the viable cell surface, but its exposure increased rapidly after induction of apoptosis, as also reported for other cell types.[26,27,42] As observed by immunofluorescence labeling, the C1q GR was found to colocalize partially with ectoCRT on early apoptotic cells, indicating that the two proteins are in close vicinity and suggesting that they possibly interact with each other. In light of these findings, the observation that CRT deficiency resulting from siRNA treatment induced an increase in apoptotic cell binding to C1q was quite intriguing. This prompted us to examine possible interactions between CRT and molecules that could be involved in C1q binding to apoptotic cells. Considering that PS has been shown to colocalize in membrane patches with CRT[26,42] and is also one of the apoptotic cell ligands recognized by C1q,[19] we tested the hypothesis that PS and CRT could interact with each other and thereby could modulate C1q binding to the apoptotic cell. PS was indeed found to bind to CRT, as demonstrated by SPR analysis using the polar moiety of PS and by co-sedimentation with PS vesicles. During the writing of this article, such an interaction between PS and CRT was actually elegantly demonstrated by Tarr and collaborators, who showed that the association with PS is involved in CRT externalization under apoptotic stress conditions.[43] The finding that the polar head of PS binds directly to CRT, with an affinity 10-fold higher than that determined for C1q, led us to hypothesize that CRT may actually efficiently compete with C1q for interaction with PS. This hypothesis was tested using a lipid–protein co-sedimentation assay, which indeed demonstrated that the C1q GR–PS interaction is impaired in the presence of CRT. Such a competition between CRT and C1q provides therefore a possible explanation for the increased cell binding to C1q resulting from siRNA-mediated CRT deficiency.

Together, these observations indicate that each of these three molecules (ectoCRT, C1q, and PS) is closely involved in the uptake of apoptotic cells through their location in the same restricted membrane areas and their potential mutual interactions. This strongly suggests a combinatorial role of

these molecules in the recognition step. How these molecules contribute to the cell–cell interaction and/or to the signaling pathways involved in the uptake process and the establishment of the new phagocyte "immunological status" remains, however, to be investigated in detail.

Whether the phagocyte CRT, a soluble extracellular form of CRT, or both are involved, directly or with the assistance of phagocyte receptors, in the formation of the phagocytic synapse is another important point that needs clarification. Indeed, several recently published studies raise additional questions. On one hand, the phagocyte CRT coreceptor CD91/LRP has been reported not to be always required for C1q-triggered enhancement of phagocytosis.[44–46] On the other hand, we have recently demonstrated a direct interaction between CD91 and C1q, which involves both the CLF and the GR domains of C1q.[47] In addition, the apoptotic cell ectoCRT could possibly interact with the phagocyte membrane through its binding to CD91 or other receptors, directly or through bridging molecules such as C1q, thereby leading to a specific signaling cascade.[26,42]

In conclusion, our results provide new insights into the role of C1q and CRT in the removal of apoptotic cells by phagocytes. They strongly suggest that complex multimolecular interactions involving at least PS, C1q, and CRT and taking place in restricted membrane areas are responsible for connecting the two types of cells and for triggering further signaling events. The unique ability of C1q to sense multiple molecular motifs[48–50] leads us to postulate that other as yet unidentified C1q partners could be involved in this process.

Materials and Methods

Proteins, antibodies, and lipids

C1q was purified from human serum, and its GR and CLF were prepared and quantified as described previously.[10,51] PS was from Sigma (L'Isle d'Abeau, France). 06:0 PS, 06:0 PC, and 06:0 PE were obtained from Avanti Polar Lipids, Inc. (Coger, Paris). Human plCRT was purified as described.[52] PA1-902A, a chicken polyclonal antibody directed against the N terminus of CRT, was obtained from Affinity Bioreagents, Inc. NB120-2908, a chicken polyclonal antibody directed against the C terminus of CRT, was from Novus Biologicals, Inc. The mouse monoclonal anti-CRT SPA-601 was obtained from Stressgen.

Cells

HeLa cells (American Type Culture collection, # CCL-2) were cultivated in Glutamax DMEM (Dulbecco's modified Eagle's medium; Invitrogen, Cergy Pontoise, France) supplemented with 10% (v/v) fetal calf serum, penicillin (2.5 U/ml), and streptomycin (2.5 μg/ml) (Invitrogen). Apoptosis was induced and quantified as described previously.[19,20] Briefly, cells were grown in sterile dishes overnight to 60–80% confluence and exposed to UV-B irradiation (1000 mJ/cm²) at 312 nm in fresh DMEM. Cells were then incubated for the indicated times at 37 °C under 5% CO_2.

Expression of the P and globular domains of CRT

All expression plasmids were derived from pHFX-CRT, a plasmid containing the cDNA encoding full-length human CRT (AU6-F11 IMAGE clone, Mammalian Gene Collection, MRC Gene Service, Cambridge, UK) fused to a HAT tag at its N terminus (N. Larsen, Structural and physicochemical properties of the chaperone protein calreticulin, thesis, University of Copenhagen, 2005). The expression plasmids for the P and globular domains were constructed by site-directed mutagenesis according to the manufacturer's instructions (QuikChange XL site-directed mutagenesis kit, Stratagene). For expression of the P domain, the N-terminal (residues 1–188) and C-terminal (residues 289–400) regions of CRT were successively deleted with the following respective primers: 5′-CAACAAGGGTTCCATCGAGGGTAG-A**AAGAAGATAAAGGATCCTGATG**-3′ and reverse; 5′-**GTATTCTCCCGATCCCAGTATC**TAAGCTT-GCGGCCGCACTCGAGC-3′ and reverse (P domain shown in bold). The expression plasmid for the globular domain was obtained by replacing residues 215–311 by a three-residue linker (GSG) with the following primers: 5′-GGAAGACGATTGGGACTTCCTGCCA**GGCTCTGGC-**GATCCCAGTATCTATGCCTATG-3′ and reverse (linker shown in bold). BL21(DE3)pLysS cells transformed with the different pHFX plasmids were optimally grown at 37 °C, and protein production was induced by 1 mM IPTG for 3 h 30 min at 37 °C. Cells were then lysed by sonication in the affinity chromatography buffer (50 mM Na_2HPO_4, 300 mM NaCl, pH 8.0) containing 1 mM DFP (diisopropyl fluorophosphate). Cell lysates were then centrifuged, filtered, and applied to a cobalt–Sepharose affinity column (TALON metal affinity resins, Clontech). After elution with 150 mM imidazole, fractions containing full-length CRT, the P domain, or the globular domain were pooled. Further purification was achieved by ion-exchange chromatography. Pooled fractions from the affinity chromatography step were dialyzed against 20 mM Tris–HCl (pH 7.5; for the P and globular domains) containing 350 mM NaCl (for full-length CRT), filtered, and applied to a monoQ5/50 GL column (Amersham Biosciences). Proteins were eluted by a 0–1 M NaCl gradient in 20 mM Tris–HCl (pH 7.5).

Electron microscopy

The binding of CRT to C1q was visualized by negative staining and transmission electron microscopy (TEM). Histidine-tagged CRT was conjugated to nickel (II)–nitrilotriacetic acid–Nanogold® (Nanoprobes). C1q molecules alone, CRT molecules alone, and mixtures of C1q and CRT molecules were incubated with gold beads at 22 °C for 40 min. About 2–4 μl of the resulting solutions was applied to carbon-coated mica sheets. The carbon films on the mica sheets were subsequently

floated in 100–200 μl of 2% sodium silicotungstate at pH 7.4 and picked up by TEM grids. The grids were observed under a Philips CM12 electron microscope at 120 kV. Images were taken with low-dose imaging and recorded with a Gatan Orius™ CCD (charge-coupled device) camera.

SPR spectroscopy

Analyses were carried out on a BIAcore 3000 or BIAcore X instrument (GE Healthcare). (i) Analyses on C1q, CRT, or CRT-fragment-coated surfaces: C1q immobilization was performed as described previously.[19] The running buffer for immobilization of CRT and its globular and P domains was 145 mM NaCl, 5 mM EDTA (ethylenediaminetetraacetic acid), and 10 mM Hepes (pH 7.4). CRT, its P domain, and its globular domain were diluted in 10 mM formate (pH 3.0) to 50, 15, and 15 μg/ml, respectively, and immobilized onto a CM5 sensor chip using the amine coupling kit (BIAcore). Binding of C1q, its GR, and its CLF to CRT and its domains was measured at a flow rate of 20 μl/min in 50 mM Tris–HCl, 150 mM NaCl, and 2 mM $CaCl_2$ containing 0.005% surfactant P20 (pH 7.4). Surfaces were regenerated by injection of 10 μl of 10 mM NaOH. The specific binding signal shown was obtained by subtracting the background signal, routinely obtained by injection of the sample over an activated–deactivated surface. All data were analyzed by global fitting either to a two-state reaction binding model or to a 1:1 Langmuir binding model of both the association and the dissociation phases for several concentrations simultaneously, using the BIAevaluation 3.2 software (BIAcore). In each case, the data presented were obtained with a statistic χ^2 value <2. For the two-state reaction binding model, the dissociation constants were calculated from the $(k_{d1}/k_{a1})(k_{d2}/k_{a2})$ ratios. For the Langmuir binding model, the apparent equilibrium dissociation constants (K_D) were calculated from the ratio of the dissociation and association rate constants (k_d/k_a). (ii) Binding of 06:0 PS, 06:0 PC, and 06:0 PE to immobilized CRT was performed as described previously for binding of 06:0 PS to immobilized C1q.[19] (iii) Analyses using viable or apoptotic cells were performed as described previously.[19,20] When necessary, untreated cells as well as cells treated with CRT siRNA were induced to undergo apoptosis prior to injection over immobilized C1q.

RNA interference

We used the 21-nucleotide sense (5′-CAUGAGCAGAACAUCGACUdTdT-3′) and antisense (5′-AGUCGAUGUUCUGCUCAUGdTdT-3′) strands of CRT mRNA (GenBank™ accession number M84739) as described by Harada *et al.*[53] As negative controls, the complementary inverse sequences, 5′-UCAGCUACAAGACGAGUACdTdT-3′ and 5′-GUACUCGUCUUGUAGCUGAdTdT-3′, were used. Heteroduplexes were prepared according to the manufacturer's protocol (Eurogentec) with a thermocycler. HeLa cells were transfected by siRNA at a final concentration of 10 nM with lipofectamine RNAiMAX (Invitrogen), following the instructions of the manufacturer. Forty-eight hours after transfection, HeLa cells were harvested and either assessed for their total CRT content by Western blotting or biotinylated and assessed for surface-exposed CRT.

Biotinylation of cell-surface proteins

Forty-eight hours after transfection, trypsinized HeLa cells were washed three times with phosphate-buffered saline (PBS) and cell-surface proteins were biotinylated with EZ-link sulfo-NHS biotin (0.5 mg/ml; Pierce) in ice-cold PBS (pH 8.0). After incubation at 4 °C for 1 h with gentle shaking, cells were washed once with ice-cold PBS containing 100 mM glycine for 10 min at 4 °C to quench unreacted biotin. Cells were then rinsed twice with ice-cold PBS, pelleted by centrifugation, and then assessed for surface-exposed CRT as described below.

Measurement of surface-exposed CRT

Cells were lysed in 1% Triton X-100 in PBS containing 1 mM $CaCl_2$, 1 mM $MgCl_2$, and protease inhibitors for 1 h at 4 °C. Insoluble material was removed by centrifugation at 14,000 rpm for 30 min at 4 °C. The supernatant was then collected and its protein concentration was measured with the bicinchoninic acid protein assay (Pierce) and adjusted to 1 μg/μl with the lysis buffer. Three hundred microliters of the supernatant was incubated with 150 μl of streptavidin-conjugated magnetic beads (Dynabeads MyOne Streptavidin T1; Invitrogen Dynal AS, Oslo, Norway) under rotation overnight at 4 °C. The beads were collected with a magnet and washed twice with PBS–0.1% Tween 20 and four times with the lysis buffer. To elute biotinylated proteins, the beads were incubated with 35 μl of Laemmli sample buffer[54] for 5 min at 100 °C. The amount of surface-exposed CRT was determined by Western blotting as described below.

SDS–PAGE and Western blotting

Equivalent amounts of soluble proteins were separated on 10% SDS-PAGE gels under reducing conditions and transferred to nitrocellulose membranes.[54] The membranes were blocked by incubation with PBS containing 0.1% Tween 20 and 5% nonfat dry milk. The membranes were then probed overnight at 4 °C with either NB120-2908 or SPA-601 as a primary antibody and washed in PBS containing 0.1% Tween 20. They were subsequently incubated for 1 h at room temperature with horseradish-peroxidase-conjugated secondary antibodies, washed thoroughly, stained with enhanced chemiluminescence reagent (Supersignal West Pico Chemiluminescent substrate, Pierce), and exposed to an X-ray film.

Co-sedimentation analyses

PS vesicles (100 μg in 100 μl PBS, 1 mM $CaCl_2$, pH 7.4) were obtained by treatment for 20 min in a bath sonicator[55] and incubated for 2 h with either rCRT (21 μg) or buffer alone. The C1q GR (10 μg in PBS, 1 mM $CaCl_2$, pH 7.4) was incubated with each vesicle sample for 30 min at 22 °C. Samples were centrifuged at 300,000*g* for 30 min at 4 °C, allowing separation of the supernatant

from the lipid-containing pellet. The protein contents of the supernatant and pellet fractions were determined by means of a 14% SDS-PAGE analysis followed by Coomassie blue staining.

Flow cytometry

HeLa cells were harvested with trypsin–EDTA (Invitrogen) at varying times after irradiation. To analyze the whole apoptotic cell population, nonadherent cells present in the culture medium were added to harvested cells. Cells (0.5×10^6/ml) were suspended in PBS containing 1% bovine serum albumin (pH 7.4), incubated for 45 min on ice with the anti-CRT antibody PA1-902A (Affinity Bioreagents, Inc.) diluted 1:100 or a control isotype, washed twice, resuspended in PBS, and incubated on ice for 30 min with donkey anti-chicken DyLight 488 (Jackson Immunoresearch, Interchim) diluted 1:200. Cells were then washed twice, resuspended in PBS, fixed with 4% paraformaldehyde for 15 min on ice, and analyzed with a FACScan flow cytometer using the CellQuest software (Becton-Dickinson).

Confocal laser scanning microscopy

HeLa cells were incubated with C1q GR (100 μg/ml) in 140 mM NaCl, 5 mM KCl, 1 mM $MgCl_2$, 2.5 mM $CaCl_2$, bovine serum albumin (1 mg/ml), and 25 mM Hepes (pH 7.4) for 1 h at 4 °C. Cells were then washed in the Hepes buffer and fixed for 5 min with 4% paraformaldehyde. CRT and bound C1q GR were then detected by indirect immunofluorescence with the anti-CRT antibody PA1-902A (10 μg/ml) and a rabbit polyclonal anti-C1q antibody diluted 1:2000, respectively. Bound antibodies were visualized with cyanine-3-conjugated donkey anti-chicken IgY diluted 1:200 and fluorescein isothiocyanate (FITC)-conjugated goat anti-rabbit IgG diluted 1:200 (both from Jackson Immunoresearch, Interchim). DNA was then stained with Hoechst dye (1 μg/ml; Sigma), and cells were mounted on glass slides with DABCO [1,4-diazabicyclo (2,2,2)octane, 25 mg/ml; Sigma] in a PBS/glycerol 1:9 (v/v) solution. Cells were photographed with a laser confocal fluorescence microscope (Leica). To assess spatial localizations within the cell and at the surface, serial optical sections were taken at 0.7-μm intervals throughout the thickness of all cells examined.

Other methods

CD measurements were carried out with a CD6 Jobin-Yvon spectropolarimeter. A 1-mm path-length cuvette was used to record the spectra. MALDI-TOF mass spectrometry analyses were performed with an Autoflex Bruker Daltonics mass spectrometer.

Acknowledgements

We thank Isabelle Bally, Guy Schoehn, Luca Signor, and Izabel Bérard from the IBS platform of the Partnership for Structural Biology and the Institut de Biologie Structurale in Grenoble (PSB/IBS) for assistance and access to the BIAcore, electron microscopy, and mass spectrometry facilities, respectively.

We thank Pierre Gans for expertise with CD, Didier Grunwald for confocal microscopy, Thomas Lunardi for purification of C1q GR, and Mickael Jacquet for technical help. We are grateful to Dr. Nicole Thielens for critical reading of the manuscript and helpful assistance with SPR analysis.

References

1. Savill, J., Dransfield, I., Gregory, C. & Haslett, C. (2002). A blast from the past: clearance of apoptotic cells regulates immune responses. *Nat. Rev. Immunol.* **2**, 965–975.
2. Ravichandran, K. S. & Lorenz, U. (2007). Engulfment of apoptotic cells: signals for a good meal. *Nat. Rev. Immunol.* **7**, 964–974.
3. Paidassi, H., Tacnet-Delorme, P., Arlaud, G. J. & Frachet, P. (2009). How phagocytes track down and respond to apoptotic cells. *Crit. Rev. Immunol.* **29**, 111–130.
4. Erwig, L. P. & Henson, P. M. (2008). Clearance of apoptotic cells by phagocytes. *Cell Death Differ.* **15**, 243–250.
5. Biro, A., Thielens, N. M., Cervenak, L., Prohaszka, Z., Fust, G. & Arlaud, G. J. (2007). Modified low density lipoproteins differentially bind and activate the C1 complex of complement. *Mol. Immunol.* **44**, 1169–1177.
6. Blanquet-Grossard, F., Thielens, N. M., Vendrely, C., Jamin, M. & Arlaud, G. J. (2005). Complement protein C1q recognizes a conformationally modified form of the prion protein. *Biochemistry*, **44**, 4349–4356.
7. Klein, M. A., Kaeser, P. S., Schwarz, P., Weyd, H., Xenarios, I., Zinkernagel, R. M. *et al.* (2001). Complement facilitates early prion pathogenesis. *Nat. Med.* **7**, 488–492.
8. Korb, L. C. & Ahearn, J. M. (1997). C1q binds directly and specifically to surface blebs of apoptotic human keratinocytes: complement deficiency and systemic lupus erythematosus revisited. *J. Immunol.* **158**, 4525–4528.
9. Navratil, J. S., Watkins, S. C., Wisnieski, J. J. & Ahearn, J. M. (2001). The globular heads of C1q specifically recognize surface blebs of apoptotic vascular endothelial cells. *J. Immunol.* **166**, 3231–3239.
10. Tacnet-Delorme, P., Chevallier, S. & Arlaud, G. J. (2001). β-Amyloid fibrils activate the C1 complex of complement under physiological conditions: evidence for a binding site for Aβ on the C1q globular regions. *J. Immunol.* **167**, 6374–6381.
11. Biro, A., Ling, W. L. & Arlaud, G. J. (2010). Complement protein C1q recognizes enzymatically modified low-density lipoprotein through unesterified fatty acids generated by cholesterol esterase. *Biochemistry*, **49**, 2167–2176.
12. Fraser, D. A., Laust, A. K., Nelson, E. L. & Tenner, A. J. (2009). C1q differentially modulates phagocytosis and

cytokine responses during ingestion of apoptotic cells by human monocytes, macrophages, and dendritic cells. *J. Immunol.* **183**, 6175–6185.
13. Fraser, D. A., Pisalyaput, K. & Tenner, A. J. (2010). C1q enhances microglial clearance of apoptotic neurons and neuronal blebs, and modulates subsequent inflammatory cytokine production. *J. Neurochem.* **112**, 733–743.
14. Hosszu, K. K., Santiago-Schwarz, F., Peerschke, E. I. & Ghebrehiwet, B. (2010). Evidence that a C1q/C1qR system regulates monocyte-derived dendritic cell differentiation at the interface of innate and acquired immunity. *Innate Immun.* **16**, 115–127.
15. Lood, C., Gullstrand, B., Truedsson, L., Olin, A. I., Alm, G. V., Ronnblom, L. *et al.* (2009). C1q inhibits immune complex–induced interferon-α production in plasmacytoid dendritic cells: a novel link between C1q deficiency and systemic lupus erythematosus pathogenesis. *Arthritis Rheum.* **60**, 3081–3090.
16. Csomor, E., Bajtay, Z., Sandor, N., Kristof, K., Arlaud, G. J., Thiel, S. & Erdei, A. (2007). Complement protein C1q induces maturation of human dendritic cells. *Mol. Immunol.* **44**, 3389–3397.
17. Castellano, G., Trouw, L. A., Fiore, N., Daha, M. R., Schena, F. P. & van Kooten, C. (2010). Infiltrating dendritic cells contribute to local synthesis of C1q in murine and human lupus nephritis. *Mol. Immunol.* **47**, 2129–2137.
18. Castellano, G., Woltman, A. M., Schlagwein, N., Xu, W., Schena, F. P., Daha, M. R. & van Kooten, C. (2007). Immune modulation of human dendritic cells by complement. *Eur. J. Immunol.* **37**, 2803–2811.
19. Paidassi, H., Tacnet-Delorme, P., Garlatti, V., Darnault, C., Ghebrehiwet, B., Gaboriaud, C. *et al.* (2008). C1q binds phosphatidylserine and likely acts as a multiligand-bridging molecule in apoptotic cell recognition. *J. Immunol.* **180**, 2329–2338.
20. Paidassi, H., Tacnet-Delorme, P., Lunardi, T., Arlaud, G. J., Thielens, N. M. & Frachet, P. (2008). The lectin-like activity of human C1q and its implication in DNA and apoptotic cell recognition. *FEBS Lett.* **582**, 3111–3116.
21. Radic, M., Marion, T. & Monestier, M. (2004). Nucleosomes are exposed at the cell surface in apoptosis. *J. Immunol.* **172**, 6692–6700.
22. Elward, K., Griffiths, M., Mizuno, M., Harris, C. L., Neal, J. W., Morgan, B. P. & Gasque, P. (2005). CD46 plays a key role in tailoring innate immune recognition of apoptotic and necrotic cells. *J. Biol. Chem.* **280**, 36342–36354.
23. Johnson, S., Michalak, M., Opas, M. & Eggleton, P. (2001). The ins and outs of calreticulin: from the ER lumen to the extracellular space. *Trends Cell. Biol.* **11**, 122–129.
24. Michalak, M., Groenendyk, J., Szabo, E., Gold, L. I. & Opas, M. (2009). Calreticulin, a multi-process calcium-buffering chaperone of the endoplasmic reticulum. *Biochem. J.* **417**, 651–666.
25. Michalak, M. & Opas, M. (2009). Endoplasmic and sarcoplasmic reticulum in the heart. *Trends Cell. Biol.* **19**, 253–259.
26. Gardai, S. J., McPhillips, K. A., Frasch, S. C., Janssen, W. J., Starefeldt, A., Murphy-Ullrich, J. E. *et al.* (2005). Cell-surface calreticulin initiates clearance of viable or apoptotic cells through trans-activation of LRP on the phagocyte. *Cell*, **123**, 321–334.
27. Obeid, M., Tesniere, A., Ghiringhelli, F., Fimia, G. M., Apetoh, L., Perfettini, J. L. *et al.* (2007). Calreticulin exposure dictates the immunogenicity of cancer cell death. *Nat. Med.* **13**, 54–61.
28. Fraser, D. A. & Tenner, A. J. (2008). Directing an appropriate immune response: the role of defense collagens and other soluble pattern recognition molecules. *Curr. Drug Targets*, **9**, 113–122.
29. Ogden, C. A., deCathelineau, A., Hoffmann, P. R., Bratton, D., Ghebrehiwet, B., Fadok, V. A. & Henson, P. M. (2001). C1q and mannose binding lectin engagement of cell surface calreticulin and CD91 initiates macropinocytosis and uptake of apoptotic cells. *J. Exp. Med.* **194**, 781–795.
30. Vandivier, R. W., Ogden, C. A., Fadok, V. A., Hoffmann, P. R., Brown, K. K., Botto, M. *et al.* (2002). Role of surfactant proteins A, D, and C1q in the clearance of apoptotic cells in vivo and in vitro: calreticulin and CD91 as a common collectin receptor complex. *J. Immunol.* **169**, 3978–3986.
31. Kishore, U., Sontheimer, R. D., Sastry, K. N., Zaner, K. S., Zappi, E. G., Hughes, G. R. *et al.* (1997). Release of calreticulin from neutrophils may alter C1q-mediated immune functions. *Biochem. J.* **322**(Pt 2), 543–550.
32. Kovacs, H., Campbell, I. D., Strong, P., Johnson, S., Ward, F. J., Reid, K. B. & Eggleton, P. (1998). Evidence that C1q binds specifically to CH2-like immunoglobulin gamma motifs present in the autoantigen calreticulin and interferes with complement activation. *Biochemistry*, **37**, 17865–17874.
33. Stuart, G. R., Lynch, N. J., Lu, J., Geick, A., Moffatt, B. E., Sim, R. B. & Schwaeble, W. J. (1996). Localisation of the C1q binding site within C1q receptor/calreticulin. *FEBS Lett.* **397**, 245–249.
34. Steino, A., Jorgensen, C. S., Laursen, I. & Houen, G. (2004). Interaction of C1q with the receptor calreticulin requires a conformational change in C1q. *Scand. J. Immunol.* **59**, 485–495.
35. Tan, Y., Chen, M., Li, Z., Mabuchi, K. & Bouvier, M. (2006). The calcium- and zinc-responsive regions of calreticulin reside strictly in the N-/C-domain. *Biochim. Biophys. Acta*, **1760**, 745–753.
36. Li, Z., Stafford, W. F. & Bouvier, M. (2001). The metal ion binding properties of calreticulin modulate its conformational flexibility and thermal stability. *Biochemistry*, **40**, 11193–11201.
37. Young, P. J., Szestakowska, D., Morse, R., Winyard, P. G., Whatmore, J., Reid, K. B. *et al.* (2006). Purification, isolation and characterization of native and recombinant calreticulin. *Calcium Binding Proteins*, **1**, 160–169.
38. Stuart, G. R., Lynch, N. J., Day, A. J., Schwaeble, W. J. & Sim, R. B. (1997). The C1q and collectin binding site within C1q receptor (cell surface calreticulin). *Immunopharmacology*, **38**, 73–80.
39. Kishore, U., Sontheimer, R. D., Sastry, K. N., Zappi, E. G., Hughes, G. R., Khamashta, M. A. *et al.* (1997). The systemic lupus erythematosus (SLE) disease autoantigen-calreticulin can inhibit C1q association with immune complexes. *Clin. Exp. Immunol.* **108**, 181–190.
40. Ellgaard, L., Riek, R., Braun, D., Herrmann, T., Helenius, A. & Wuthrich, K. (2001). Three-dimensional

structure topology of the calreticulin P-domain based on NMR assignment. *FEBS. Lett.* **488**, 69–73.
41. Ellgaard, L., Riek, R., Herrmann, T., Guntert, P., Braun, D., Helenius, A. & Wuthrich, K. (2001). NMR structure of the calreticulin P-domain. *Proc. Natl Acad. Sci. USA*, **98**, 3133–3138.
42. Gardai, S. J., Bratton, D. L., Ogden, C. A. & Henson, P. M. (2006). Recognition ligands on apoptotic cells: a perspective. *J. Leukoc. Biol.* **79**, 896–903.
43. Tarr, J. M., Young, P. J., Morse, R., Shaw, D. J., Haigh, R., Petrov, P. G. *et al.* (2010). A mechanism of release of calreticulin from cells during apoptosis. *J. Mol. Biol.* **401**, 799–812.
44. Kozmar, A., Greenlee-Wacker, M. C. & Bohlson, S. S. (2010). Macrophage response to apoptotic cells varies with the apoptotic trigger and is not altered by a deficiency in LRP expression. *J. Innate. Immun.* **2**, 248–259.
45. Lillis, A. P., Greenlee, M. C., Mikhailenko, I., Pizzo, S. V., Tenner, A. J., Strickland, D. K. & Bohlson, S. S. (2008). Murine low-density lipoprotein receptor-related protein 1 (LRP) is required for phagocytosis of targets bearing LRP ligands but is not required for C1q-triggered enhancement of phagocytosis. *J. Immunol.* **181**, 364–373.
46. Donnelly, S., Roake, W., Brown, S., Young, P., Naik, H., Wordsworth, P. *et al.* (2006). Impaired recognition of apoptotic neutrophils by the C1q/calreticulin and CD91 pathway in systemic lupus erythematosus. *Arthritis Rheum.* **54**, 1543–1556.
47. Duus, K., Hansen, E. W., Tacnet, P., Frachet, P., Arlaud, G. J., Thielens, N. M. & Houen, G. (2010). Direct interaction between CD91 and C1q. *FEBS J.* **277**, 3526–3537.
48. Gaboriaud, C., Juanhuix, J., Gruez, A., Lacroix, M., Darnault, C., Pignol, D. *et al.* (2003). The crystal structure of the globular head of complement protein C1q provides a basis for its versatile recognition properties. *J. Biol. Chem.* **278**, 46974–46982.
49. Garlatti, V., Chouquet, A., Lunardi, T., Vives, R., Paidassi, H., Lortat-Jacob, H. *et al.* (2010). Cutting edge: C1q binds deoxyribose and heparan sulfate through neighboring sites of its recognition domain. *J. Immunol.* **185**, 808–812.
50. Kishore, U., Gaboriaud, C., Waters, P., Shrive, A. K., Greenhough, T. J., Reid, K. B. *et al.* (2004). C1q and tumor necrosis factor superfamily: modularity and versatility. *Trends Immunol.* **25**, 551–561.
51. Arlaud, G. J., Sim, R. B., Duplaa, A. M. & Colomb, M. G. (1979). Differential elution of Clq, Clr and Cls from human Cl bound to immune aggregates. Use in the rapid purification of Cl subcomponents. *Mol. Immunol.* **16**, 445–450.
52. Houen, G. & Koch, C. (1994). Human placental calreticulin: purification, characterization and association with other proteins. *Acta Chem. Scand.* **48**, 905–911.
53. Harada, K., Okiyoneda, T., Hashimoto, Y., Ueno, K., Nakamura, K., Yamahira, K. *et al.* (2006). Calreticulin negatively regulates the cell surface expression of cystic fibrosis transmembrane conductance regulator. *J. Biol. Chem.* **281**, 12841–12848.
54. Laemmli, U. K. (1970). Cleavage of structural proteins during the assembly of the head of bacteriophage T4. *Nature*, **227**, 680–685.
55. Ishii, M., Fujita, S., Yamada, M., Hosaka, Y. & Kurachi, Y. (2005). Phosphatidylinositol 3,4,5-trisphosphate and Ca^{2+}/calmodulin competitively bind to the regulators of G-protein-signalling (RGS) domain of RGS4 and reciprocally regulate its action. *Biochem. J.* **385**, 65–73.